NEOPLASIA
www.neoplasia.com

Volume 21 Number 4 April 2019 pp. 376–388 376

Preclinical Prevention Trial of Calcitriol: Impact of Stage of Intervention and Duration of Treatment on Oral Carcinogenesis

Vui King Vincent-Chong[*], Hendrik DeJong[*], Kristopher Attwood[†], Pamela A. Hershberger[‡] and Mukund Seshadri[*,§]

[*]Department of Oral Oncology, Roswell Park Comprehensive Cancer Center, Buffalo, New York 14263; [†]Department of Biostatistics and Bioinformatics, Roswell Park Comprehensive Cancer Center, Buffalo, New York 14263; [‡]Department of Pharmacology and Therapeutics, Roswell Park Comprehensive Cancer Center, Buffalo, New York 14263; [§]Department of Dentistry and Maxillofacial Prosthetics, Roswell Park Comprehensive Cancer Center, Buffalo, New York 14263

Abstract

The anticancer activity of 1,25-dihydroxyvitamin D3 (1,25$(OH)_2D_3$ or calcitriol) has been widely reported in preclinical models. However, systematic investigation into the chemopreventive potential of calcitriol against the spectrum of oral carcinogenesis has not been performed. To address this gap in knowledge, we conducted a preclinical prevention trial of calcitriol in the 4-nitroquinoline-1-oxide (4NQO) oral carcinogenesis model. C57BL/6 mice were exposed to the carcinogen 4NQO in drinking water for 16 weeks and randomized to control (4NQO only) or calcitriol arms. Calcitriol (0.1 μg i.p, Monday, Wednesday, and Friday) was administered for (i) 16 weeks concurrently with 4NQO exposure, (ii) 10 weeks post completion of 4NQO exposure, and, (iii) a period of 26 weeks concurrent with and following 4NQO exposure. Longitudinal magnetic resonance imaging (MRI) was performed to monitor disease progression until end point (week 26). Correlative histopathology of tongue sections was performed to determine incidence and multiplicity of oral dysplastic lesions and squamous cell carcinomas (SCC). Vitamin D metabolites and calcium were measured in the serum using liquid chromatography-mass spectrometry (LC–MS/MS) and colorimetric assay, respectively. Renal CYP24A1 (24-hydroxylase) and CYP27B1 (1α-hydroxylase) expression was measured by quantitative reverse transcription polymerase chain reaction (qRT-PCR). Immunostaining of tongue sections for vitamin D receptor (VDR), CYP24A1, and Ki67 was also performed. Non-invasive MRI enabled longitudinal assessment of lesions in the oral cavity. Calcitriol administered concurrently with 4NQO for 16 weeks significantly ($P < .001$) decreased the number of premalignant lesions by 57% compared to 4NQO only controls. Mice treated with calcitriol for 26 weeks showed highest renal CYP24A1, lowest serum 1,25$(OH)_2D_3$ levels and highest incidence of invasive SCC. Immunohistochemistry revealed increased VDR, CYP24A1 and Ki67 staining in dysplastic epithelia compared to normal epithelium, in all four groups. Collectively, our results show that the effects of calcitriol on oral carcinogenesis are critically influenced by the stage of intervention and duration of exposure and provide the basis for exploring the potential of calcitriol for prevention of OSCC in the clinical setting.

Neoplasia (2019) 21, 376–388

Introduction

Oral cancer is one of the major causes of cancer-related morbidity and mortality worldwide with over 90% diagnosed histologically as oral squamous cell carcinomas (OSCC) [1,2]. Development and progression of OSCC is a multi-step process that is associated with accumulation of genetic alterations over time as a result of chronic

Address all correspondence to: Dr. Mukund Seshadri, Roswell Park Comprehensive Cancer Center, Elm and Carlton streets, Buffalo, New York 14263.
Received 19 September 2018; Revised 12 February 2019; Accepted 14 February 2019

1476-5586
https://doi.org/10.1016/j.neo.2019.02.002

exposure to carcinogens such as tobacco, cigarette smoke, and alcohol [3,4]. The high rate of recurrence of OSCC and the formation of second primary tumors has been attributed to a number of factors including field cancerization, *i.e.* multifocal development of disease in the mucosa following carcinogen exposure [3–5]. This unique disease biology makes OSCC an ideal target for preventive intervention.

Vitamin D is a fat-soluble vitamin that is known to regulate several physiologic processes including skeletal function through its effects on calcium and phosphorus metabolism [6,7]. In humans, vitamin D is synthesized upon exposure to sunlight or can be obtained through dietary consumption of fortified foods and undergoes metabolic conversion in the liver and kidneys [6]. Vitamin D undergoes initial hydroxylation to 25-hydroxycholecalciferol in the liver and further hydroxylation in the kidneys by the cytochrome P450 monooxygenase CYP27B1 [1α (OH) ase] to the active metabolite, 1,25-dihydroxycholecalciferol [1,25 $(OH)_2D_3$] or calcitriol. Catabolic inactivation of 1,25 $(OH)_2D_3$ to 1,24,25 $(OH)_2D_3$ occurs in kidneys or locally in target tissues through auto-induction of the 24-hydroxylase [24(OH)ase; encoded by the CYP24A1] [6,7]. Auto-induction occurs when $1,25(OH)_2D_3$ binds to the vitamin D receptor (VDR). Ligand-activated VDR binds to vitamin D response elements (VDREs) within the CYP24A1 promoter to increase gene transcription [8,9]. CYP24A1 induction is an indicator of functional vitamin D signaling within cells [10].

In addition to its essential role in health, vitamin D status has also been linked to several pathologic conditions including hypertension, diabetes and cancer [11–13]. Epidemiologic studies have reported an inverse association between circulating levels of $25(OH)D_3$ and risk of several cancers including oral cancer [14,15]. A high prevalence of vitamin D insufficiency has also been reported in head and neck cancer patients [16]. Mechanistically, calcitriol, the active metabolite of vitamin D, exerts potent antitumor effects through inhibition of proliferation, promotion of apoptosis and blockade of angiogenesis, all of which are mediated through the vitamin D receptor (VDR) [17,18]. The chemopreventive effects of calcitriol have been documented in preclinical models of breast, prostate, lung and oral cancers [19–23]. Meier et al. have demonstrated that systemic administration of calcitriol significantly delays oral carcinogenesis in the hamster buccal pouch [22]. We have previously reported that short-term treatment with calcitriol enhances efficacy of the epidermal growth factor receptor (EGFR) inhibitor, Erlotinib, in the 4-nitroquinoline-1-oxide (4NQO) carcinogen-induced model of oral cancer [23]. While studies have demonstrated the potent growth inhibitory effects of calcitriol against oral and head and neck cancer cells *in vitro* [24,25], systematic investigation into the chemopreventive potential of calcitriol against the spectrum of oral carcinogenesis has not been performed to date. To address this gap in knowledge, in the present study, we conducted preclinical prevention trials in the 4NQO oral carcinogenesis model [26] to determine the impact of stage of intervention on the activity of calcitriol against OSCC. C57BL/6 mice were administered calcitriol concurrently with and/or following 4NQO exposure to evaluate the effect of calcitriol on disease initiation and promotion/progression of OSCC. A combination of non-invasive magnetic resonance imaging (MRI), liquid chromatography-mass spectrometry (LC–MS/MS), colorimetric assay, quantitative reverse transcription polymerase chain reaction (qRT-PCR) along with immunohistochemical and histologic evaluation was employed to examine the impact of multiple calcitriol regimens on disease progression, vitamin D metabolism and signaling.

Materials and Methods

Reagents

Calcitriol was prepared in 100% ethanol at a concentration of 200 μg/ml, stored at −80°C, and further diluted in Dulbecco's phosphate buffered saline (DPBS) to a concentration of 1 μg/ml for treatment. The carcinogen 4NQO (Sigma-Aldrich, St. Louis, MO, USA) was dissolved in propylene glycol at 4 mg/ml and diluted in autoclaved water to a final concentration of 100 μg/ml. A fresh batch of 4NQO dissolved in drinking water was prepared every week for each of the 16 weeks of carcinogenic exposure [23,27]. Regular autoclaved water was provided following completion of carcinogen exposure.

Animals, Study Design, and Endpoints

Experimental studies were carried out using 15 week old female C57BL/6NCr mice (Charles River, Wilmington, MA, USA). Animals were housed in microisolator cages with 12-hour light-and-dark cycles in the Laboratory Animal Shared Resource at Roswell Park Comprehensive Cancer Center. Animals were fed house chow that contains 1000 IU vitamin D3 throughout the entire study duration. The design for the two experimental studies is shown schematically in Figure 1.

Study 1 – Inhibition of Initiation (Figure 1A). C57BL/6 mice (n = 10 total) were administered PBS (n = 4; 4NQO) or calcitriol (n = 6; 0.1 μg i.p, Monday, Wednesday, Friday; 4NQO + calcitriol; *shaded in yellow*) concurrently with 4NQO exposure in drinking water for a total of 16 weeks. Non-invasive magnetic resonance imaging (MRI) was performed at week 0 prior to start of 4NQO exposure and at the end of week 16. Following completion of imaging, animals were euthanized for histologic evaluation of the incidence of premalignant and malignant lesions.

Study 2 – Inhibition of Progression (Figure 1B). C57BL/6 mice (n = 19 total) were randomized into a PBS control arm (n = 4; 4NQO) or one of three calcitriol arms. *Arm 1* (n = 5): Calcitriol (0.1 μg i.p, Monday, Wednesday, Friday) administered concurrently with 4NQO exposure in drinking water for a total of 16 weeks (4NQO + calcitriol; *shaded in yellow*). *Arm 2* (n = 5): Calcitriol (0.1 μg i.p, Monday, Wednesday, Friday) administered 10 weeks post completion of 16 weeks of 4NQO exposure (4NQO → calcitriol; *shaded in blue*). *Arm 3* (n = 5): Calcitriol (0.1 μg i.p, Monday, Wednesday, Friday) administered for a period of 26 weeks concurrent with and following 4NQO exposure (4NQO + calcitriol → calcitriol; *shaded in red*). Visual examination of tongue lesions was performed under white light and body weight measurements were obtained once every 3 days throughout the duration of the study as a measure of toxicity. Non-invasive magnetic resonance imaging (MRI) was performed at week 0 prior to start of 4NQO exposure with subsequent examinations performed at weeks 16, 20, 24 and 26 of study. Mice were humanely euthanized at study end point (week 26) or when animals exhibited a sustained loss of body weight (>20% of their highest body weight). At week 26, histopathologic assessment of tongue sections was performed to examine the effects of the three calcitriol regimens on the incidence of oral dysplastic lesions and squamous cell carcinomas. In addition to histologic evaluation, tongue sections were immunostained for VDR, CYP24A1 and the proliferation marker, Ki67. Serum levels of 25 $(OH)D_3$, 1,25 $(OH)_2D_3$ and calcium were determined using liquid chromatography-mass spectrometry (LC–MS/MS) and colorimetric assay, respectively. Renal CYP24A1 and CYP27B1 expression was measured by quantitative reverse transcription polymerase chain reaction (qRT-PCR). All experimental procedures were performed in accordance with approved protocols at Roswell Park Comprehensive Cancer Center.

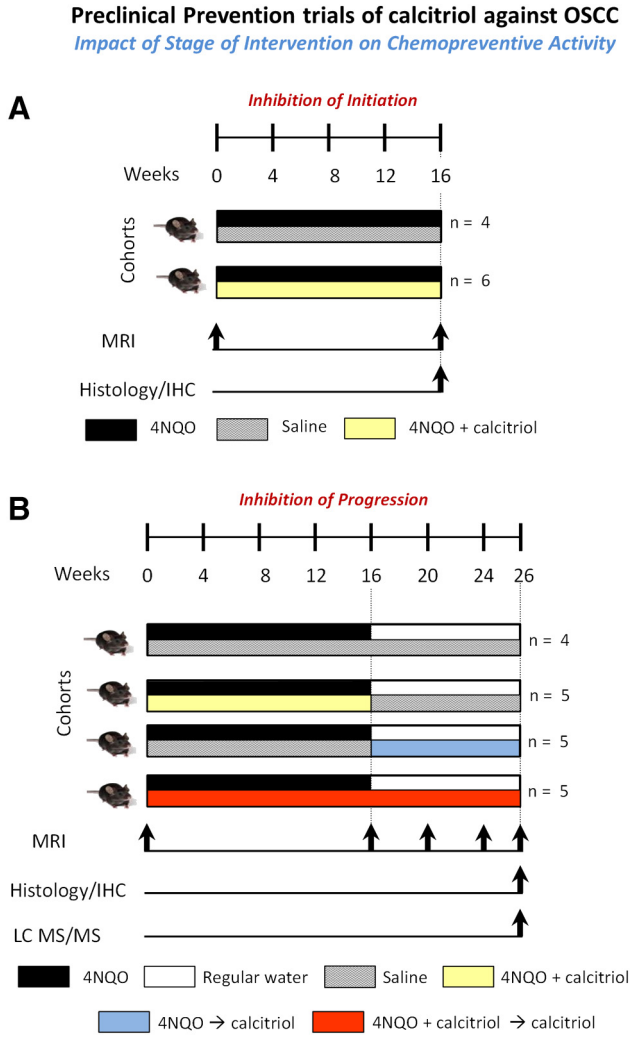

Figure 1. Preclinical prevention trials of calcitriol against OSCC. Two studies were conducted to examine the effects of calcitriol on inhibition of disease initiation (**A**) and progression (**B**) in the 4NQO model. In the first study (**A**), C57BL/6 mice were administered PBS (n = 4; 4NQO) or calcitriol (n = 6; 0.1 μg i.p, Monday, Wednesday, Friday; 4NQO + calcitriol; *shaded in yellow*) for a total of 16 weeks concurrently with 4NQO exposure in drinking water. Non-invasive magnetic resonance imaging (MRI) was performed at week 0 prior to start of 4NQO exposure and at the end of week 16. Following completion of imaging, animals were euthanized for histologic evaluation of the incidence of premalignant and malignant lesions. **(B)** In the second study, C57BL/6 mice were randomized into a PBS control arm (n = 4; 4NQO) or one of three calcitriol (0.1 μg i.p, Monday, Wednesday, Friday) arms. *Arm 1* (n = 5): Calcitriol was administered concurrently with 4NQO exposure in drinking water for a total of 16 weeks (4NQO + calcitriol; *shaded in yellow*). *Arm 2* (n = 5): Calcitriol was administered 10 weeks post completion of 16 weeks of 4NQO exposure (4NQO → calcitriol; *shaded in blue*). *Arm 3* (n = 5): Calcitriol was administered for a period of 26 weeks concurrent with and following 4NQO exposure (4NQO + calcitriol → calcitriol; *shaded in red*). Non-invasive magnetic resonance imaging (MRI) was performed at week 0 prior to start of 4NQO exposure with subsequent examinations performed at weeks 16, 20, 24 and 26 of study. At week 26, histopathologic assessment of tongue sections was performed to examine the effects of the three calcitriol regimens on the incidence of oral premalignant lesions and invasive cancer. Tongue sections were also immunostained for VDR, CYP24A1 and Ki67. Serum levels of 25 $(OH)D_3$, 1,25 $(OH)_2D_3$ and calcium were determined using liquid chromatography-mass spectrometry (LC–MS/MS) and colorimetric assay, respectively.

MRI

MRI examinations were performed using a 4.7-T/33-cm horizontal bore magnet (GE NMR Instruments) within the Translational Imaging Shared Resource at Roswell Park. Briefly, the mice were secured in an MR-compatible sled and positioned in the scanner. Animal body temperature was maintained at 37°C during imaging using an air heater system (SA Instruments Inc., Stony Brook, NY) and sensors in the sled enabled temperature and respiratory monitoring during imaging. Multi-slice axial T2-weighted (T2W) spin echo images incorporating rapid acquisition with relaxation enhancement (RARE) encoding were acquired for each mouse and analyzed as described previously [23].

Analysis of Vitamin D Metabolites

Blood samples were collected by cardiac puncture at study endpoint. Approximately 300–400 μl of whole blood per mouse was collected to isolate serum. Levels of $1,25(OH)_2D_3$, $25(OH)D_3$ and calcium were measured in sera pooled from 3–4 animals in each experimental group. Assays were performed by Heartland Assays (Ames, IA, USA).

Quantitative PCR

Kidneys were homogenized using a mortar and pestle and subjected to RNA extraction using the TRI-reagent, Direct-Zol, RNA Mini-Prep Kit (Zymo Research, Irvine, CA, USA) according to manufacturers' directions. The purity and concentration of the RNA was assessed using NanoDrop (Thermo Fisher Scientific, Waltham, MA, USA). Reverse transcription of total RNA was performed using the High Capacity cDNA reverse transcription kit with random hexamer primers (Applied Biosystems, Foster City, CA, USA). The cDNAs were quantified in triplicate and 5 ng was used to measure expression of CYP24A1 and CYP27B1 using the standard SYBR Green protocol in a 7300 Real-Time PCR System (Applied Biosystems, Foster City, CA, USA). GAPDH was amplified and served as an internal control. The primer sequences were as follows: mouse *GAPDH*: (forward) 5′ TGA GGC CGG TGC TGA GTA TGT CG 3′ and (reverse) 5′ CCA CAG TCT TCT GGG TGG CAG TG 3′; mouse CYP24A1: (forward) 5′ GCA CAA GAG CCT CAA CAC CAA 3′ and (reverse) 5′ AGA CTG TTT GCT GTC GTT TCC A 3′; mouse CYP27B1: (forward) 5′ CAG TCC ATC CTG GGA AAT GTG A 3′ and (reverse) 5′ ACC ACA GGG TAC AGT CTT AGC A 3′. The $^{\Delta\Delta}$Ct method was used to calculate relative gene expression. The 4NQO only control group was used as a reference.

Histological Assessment

Whole tongue specimens were fixed in 10% neutral-buffered formalin (Sigma-Aldrich, St. Louis, MO, USA) and longitudinally dissected for histology. Three sections 50 μm apart were stained with hematoxylin and eosin (H&E), and the worst histologic grade was identified. Histological assessment of tongue lesions was performed based on criteria suggested by Warnakulasuriya et al. [28,29]. Briefly, hyperplasia and hyperkeratosis were defined as thickened epithelium with prominent surface keratinization with or without a thickened spinous layer that exhibited an absence of nuclear atypia in the epithelial cell. Oral epithelial dysplasia was defined by evidence of increased nuclear:cytoplasmic ratio, hyperchromatic nuclei, increased or abnormal mitotic figures, nuclear pleomorphism, loss of polarity in the epithelial cells, dyskeratosis and drop-shaped rete ridges. Dysplasia was classified as 'mild' when these changes involved the lower third parabasal layers, 'moderate' when changes extended to the middle third, and as severe dysplasia or carcinoma *in situ* (CIS) when dysplastic changes were detected in the upper third layers. Papillary

lesions were characterized by moderate or severe anaplastic epithelial lesions with exophytic papillary projections and invasive cancer was defined as lesions that exhibited atypical epithelial cells in the underlying connective tissue stroma [23,27]. Mild and moderate dysplastic lesions were grouped as low grade dysplasia while severe dysplasia/CIS was considered as high grade dysplasia. Papillary lesions and invasive carcinomas were grouped as SCCs. Incidence of dysplasia and SCC was reported as percentage of animals based on worst histology from three contiguous tongue sections separated by 50 μm. Multiplicity was calculated by summing up individual lesions in each of the three sections and reported as a total number of dysplastic or SCC lesions per mouse.

Immunohistochemistry

Immunostaining of tongue sections for VDR, CYP24A1 and Ki67 was performed on formalin fixed paraffin embedded (FFPE) tongue sections using the Envision technique, Dako Real EnVision Detection System and Peroxidase/DAB+ (Agilent Technologies, Santa Clara, CA, USA) according to the manufacturer's protocol. Briefly, the FFPE sections were de-paraffinized with xylene followed by rehydration in descending grades of Ethanol. Heat mediated antigen retrieval was performed using a vegetable steamer (95–98°C, 30 minutes) in 10 mM citrate buffer (pH 6.0). Endogenous peroxidase activities were blocked with endogenous peroxidase blocking agent for 10 minutes followed by a serum-free protein block for 1 hour in room temperature. FFPE sections were incubated with antibodies specific for VDR (Thermo Fisher Scientific; MA1–710; 1:500 for 30 minutes at room temperature), CYP24A1 (MyBioSource, Inc.; MBS178241; 1:1000; 1 hour at 37°C) and Ki67 (Cell Signaling Technology; D3B5; 1:200; overnight at 4°C). For VDR immunostaining, unconjugated Rabbit Anti-Rat IgG antibody (Vector Lab, Burlingame, CA, USA) was applied for 30 minutes followed by secondary antibody (Dako, Agilent Technologies, Santa Clara, CA, USA) for another 30 minutes for VDR. Secondary antibody for CYP24A1 and Ki67 were applied for 1 hour. DAB (Diaminobenzidine) (Dako, Agilent Technologies, Santa Clara, CA, USA) was applied for 5 minutes for visualization. FFPE sections were counterstained with Harris hematoxylin, dehydrated through ethanol, cleared with xylene, and mounted. The FFPE sections were digitized using ScanScope XT system (Aperio Technologies). Quantification of nuclear VDR and cytoplasmic CYP24A1 immunoreactivity was performed at 10× magnification. Captured digital images were analyzed using the Image J IHC profiler Macro (NIH Image J, Version 1.51j8) to calculate the staining intensity. Quantitation of Ki67 immunoreactivity was performed at 40x magnification. The intensity scores were classified as: negative = 0; weak = 1; moderate = 2 and strong = 3. The proportion of Ki67+ cells was quantified as: 0 = negative; 1 = ≤10%; 2 = 11–50%; 3 = 51–80% and 4 = ≥ 80% of positive cells. The final Ki67 immune-reactive score was determined by multiplying the intensity and the proportion scores of the stained cells to obtain an immune-reactive score ranging from 0 to 12.

Statistical Analysis

Body weight measurements obtained were analyzed by comparing average weekly body weight values between control and calcitriol groups over the 26 week study period using multiple *t* tests beginning at week 0. Comparisons of multiplicity of premalignant and malignant lesions at week 26 among the groups were performed using weighted least-squares ANOVA with Tukey adjusted post-hoc comparisons. Differences in CYP24A1 and CYP27B1 mRNA expression levels between multiple groups were analyzed using one-way ANOVA with Tukey adjusted post-hoc test. Pearson's correlation analyses were performed to evaluate the relationship between duration of calcitriol exposure and (a) vitamin D metabolite, (b) calcium levels, and (c) mRNA levels of enzymes. VDR, CYP24A1 and Ki67 staining intensity data was summarized for healthy epithelium and diseased tissue (low-grade dysplasia, high-grade dysplasia and OSCC) and compared for control and calcitriol groups using Holm-Bonferroni adjusted tests. All model assumptions were verified graphically and transformations were applied as appropriate. Student's t-test, one-way ANOVA test and Pearson's correlation were performed using Graph Pad Prism version 7.00 for Windows (Graph Pad Software, La Jolla, CA, USA). Weighted least-squares ANOVA with Tukey adjusted post-hoc comparisons and Holm-Bonferroni adjusted tests were performed using SAS software (version 9.4, Cary, NC, USA). All measured values were reported as the mean ± standard error of the mean (SEM). A significance level of 0.05 was considered for all analyses.

Results

Calcitriol Inhibits Initiation of Oral Carcinogenesis in the 4NQO Model

We first examined the effect of calcitriol on the initiation of OSCC in the 4NQO model. To this end, C57BL/6 mice were randomized to receive calcitriol (n = 6; 0.1 μg i.p, Monday, Wednesday, Friday; 4NQO + calcitriol) or equal volume of PBS (n = 4; 4NQO alone) concurrently with 4NQO exposure in drinking water for a total of 16 weeks. Non-invasive magnetic resonance imaging (MRI) was performed at week 0 (prior to 4NQO exposure or calcitriol/PBS treatment) and at the end of week 16. The panel of images shown in Figure 2*A* represent axial T2-weighted (T2W) MR images of a control and a calcitriol-treated animal at week 0 and at week 16. A single slice of approximately the same anatomic region of the tongue is shown across time points for both groups. T2-weighted MRI of naïve (non-4NQO exposed mice) did not show any evidence of abnormalities or exophytic masses in the oral cavity (Supplementary Figure S1). Compared to baseline scans, 4NQO exposure over 16 weeks resulted in bilateral thickening of the lateral borders of the tongue that appeared hyperintense (*yellow arrows*) on the T2W images in animals in both control (*top*) and calcitriol (*bottom*) treated animals. No evidence of exophytic lesions in the tongue or oral cavity were detected in any of the mice on MRI during the 16 week period. Corresponding histologic sections of the tongue from the control animal showed hyperplastic squamous epithelium with moderate epithelial dysplasia, while the calcitriol treated animal showed mild dysplasia. Consistent with the absence of tongue masses on MRI, histologic evaluation did not reveal presence of invasive cancer in any of the animals. Quantification of the number of dysplastic lesions revealed a significant reduction ($P < .05$) in the number of lesions (Figure 2*B*) in the calcitriol group (13.17 ± 2.23; n = 6) compared to PBS controls (22.25 ± 2.05; n = 4).

Safety and Metabolic Profiles of Long-Term Calcitriol Administration in the 4NQO Model

Next, we investigated the safety of long-term calcitriol exposure using the three regimens in the 4NQO model. The three calcitriol regimens were well tolerated by the animals with no clinical signs of toxicity (ruffled fur, altered movement, lethargy or death) observed during the study period. In addition, body weight measurements obtained once every 3 days did not show any evidence of excessive weight loss (>20%) with the three calcitriol regimens compared to PBS controls (Figure 3*A*). At baseline (week 0) prior to start of

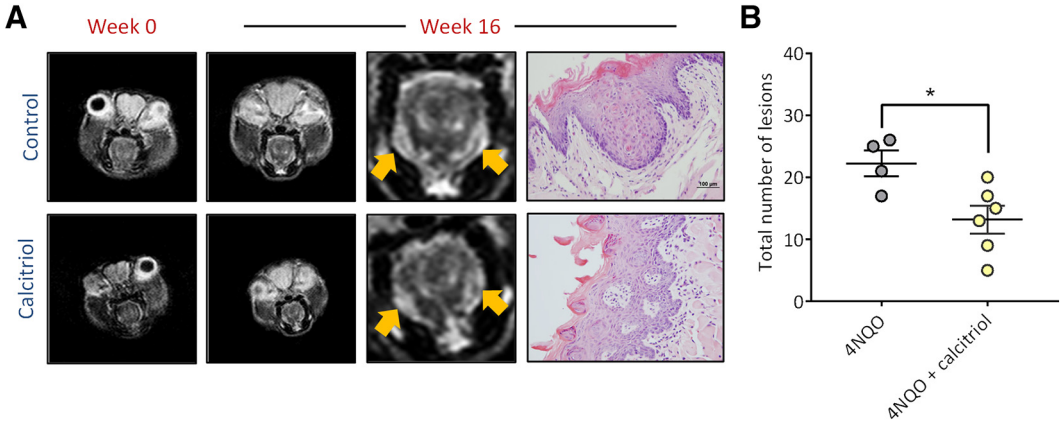

Figure 2. Calcitriol inhibits initiation of oral carcinogenesis in the 4NQO model. (**A**) Axial T2-weighted (T2W) MR images of a control and a calcitriol-treated animal at week 0 and at week 16. A single slice of approximately the same anatomic region of the tongue is shown across time points for both groups. 4NQO exposure resulted in bilateral thickening of the lateral borders of the tongue that appeared hyperintense (*yellow arrows*) on the T2W images in animals in both control (*top*) and calcitriol (*bottom*) treated animals. Corresponding histologic section of the control animal showed hyperplastic squamous epithelium with moderate epithelial dysplasia, while the calcitriol treated animal showed mild dysplasia. (**B**) Dot plot shows a significant reduction ($P < .05$) in the number of premalignant lesions with calcitriol treatment compared to PBS controls.

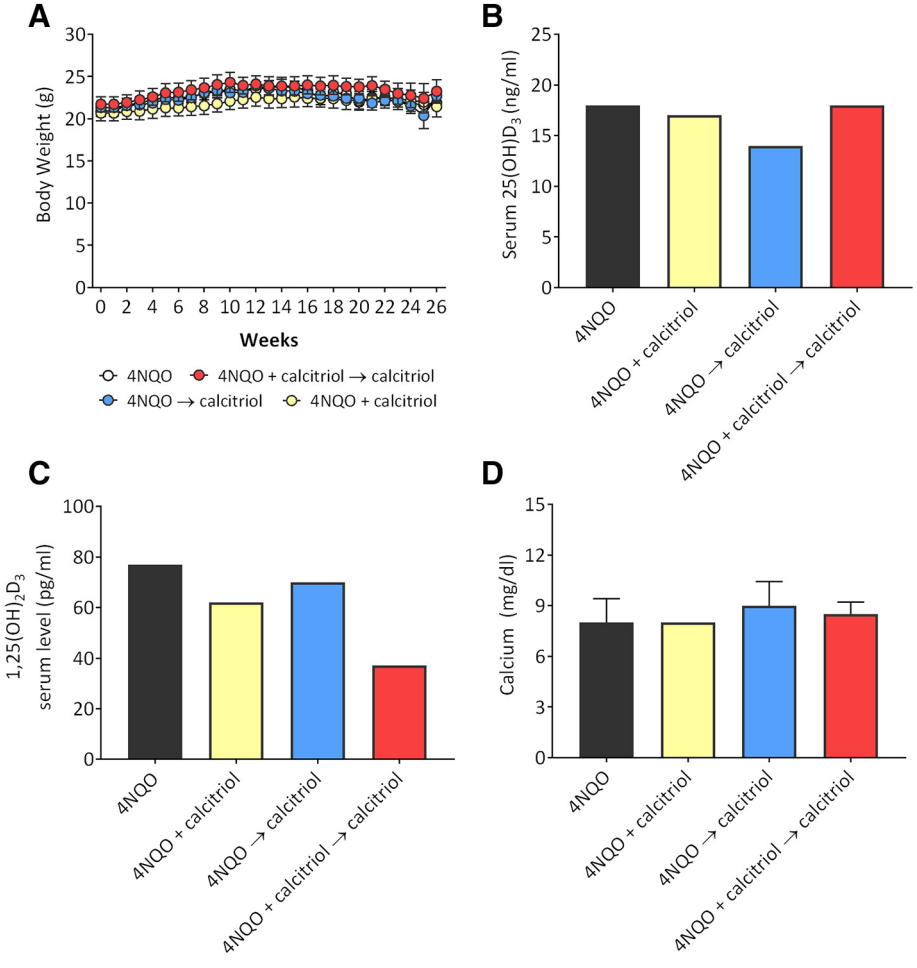

Figure 3. Safety and metabolic profiles of long term calcitriol administration in 4NQO-induced oral carcinogenesis *in vivo*. **(A)** Plot shows weekly body weight measurements of mice from all 4 experimental groups obtained as a measure of toxicity. Body weight measurements were obtained once every 3 days for the entire 26 week duration of the study. Differences in average weekly body weights are shown for animals in control arm (*white circles*), 4NQO + calcitriol (*yellow circles*), 4NQO → calcitriol (*blue circles*) and 4NQO + calcitriol → calcitriol (*red circles*). Body weight measurements remained relatively stable throughout the 26 week period with no significant difference in body weight (gain or loss) observed between control and calcitriol arms. Bar graphs show serum levels of 25(OH)D_3 (**B**) and 1,25(OH)$_2$$D_3$ (**C**) and calcium (**D**) in 4NQO controls and the three calcitriol treatment groups.

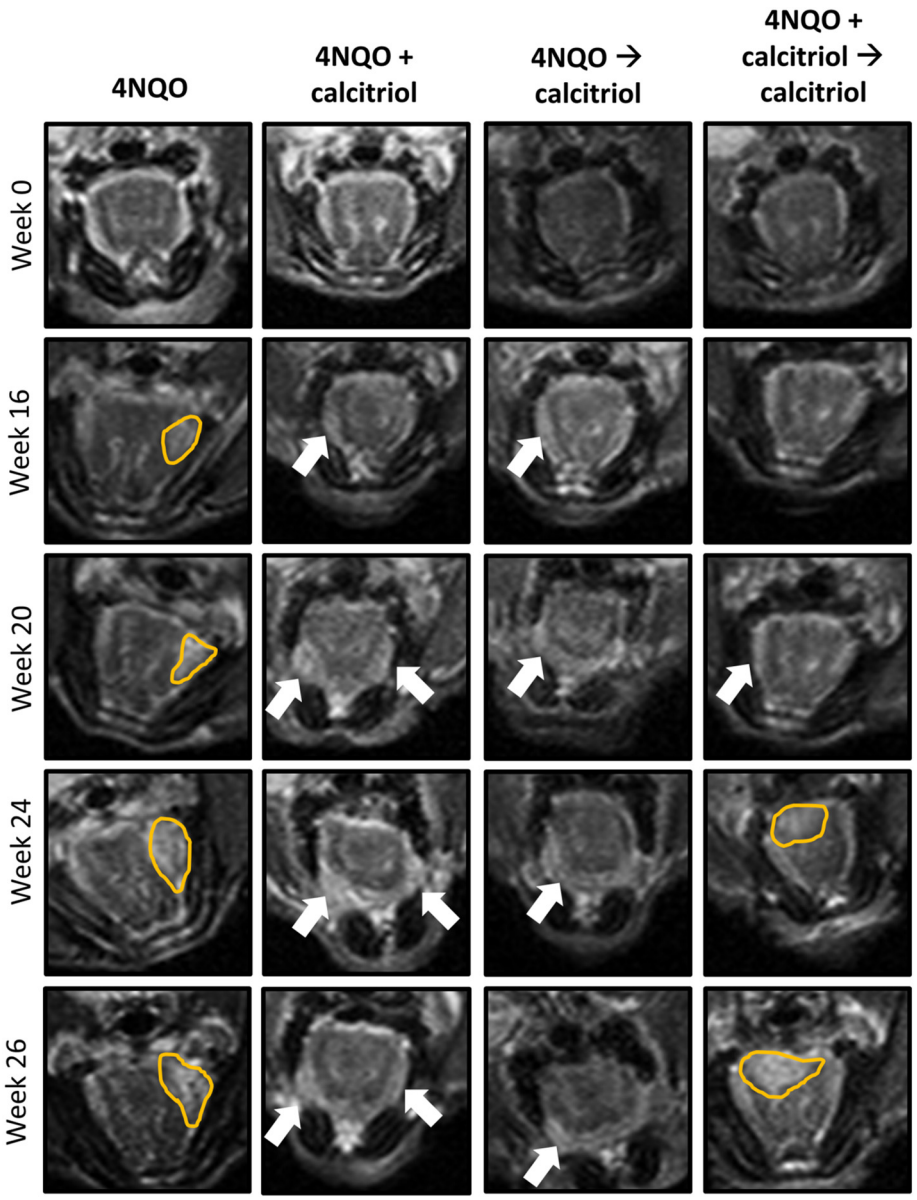

Figure 4. MRI of 4NQO-induced oral carcinogenesis *in vivo*. T2-weighted axial images of a representative C57BL/6 mouse from the control (4NQO group) and the three calcitriol treatment groups. Images are shown prior to 4NQO exposure (Week 0), 16 weeks post completion of 4NQO (Week 16) and at study end point (Week 26). The location of the exophytic oral lesions (outlined in yellow) and areas of thickening on the lateral borders of the tongue (arrows) are illustrated on the images. While exophytic lesions were seen in control, 4NQO → calcitriol and 4NQO + calcitriol → calcitriol regimens, animals treated with 4NQO + calcitriol did not show any evidence of exophytic lesions in the oral cavity on MRI.

treatment, the mean body weight of animals in the control arm was 20.8 ± 1.2 g and comparable to animals in the three calcitriol arms: 20.6 ± 2.1 g (4NQO + calcitriol), 21.3 ± 0.4 g (4NQO → calcitriol) and 21.7 ± 2.0 g (4NQO + calcitriol → calcitriol). Body weight measurements remained relatively stable throughout the 26 week period with no significant difference in body weight (gain or loss) observed between control and calcitriol arms. At week 26, the mean body weight of animals in the control arm was 21.8 ± 1.2 g, while animals in the three calcitriol arms weighed 21.4 ± 2.77 g (4NQO + calcitriol), 22.7 ± 0.98 g (4NQO → calcitriol) and 23.2 ± 2.7 g (4NQO + calcitriol → calcitriol).

To investigate the effect of the three calcitriol regimens on vitamin D homeostasis, we measured serum levels of $25(OH)D_3$ and $1,25(OH)_2D_3$ by LC–MS/MS. As shown in Figure 3*B*, $25(OH)D_3$ levels were comparable between 4NQO alone controls (18 ng/ml) and the two calcitriol regimens, 4NQO + calcitriol → calcitriol (18 ng/ml) and 4NQO + calcitriol (17 ng/ml). Mice from the 4NQO → calcitriol group exhibited slightly lower $25(OH)D_3$ levels (14 ng/ml). Lowest level of $1,25(OH)_2D_3$ (37 pg/ml) was measured in mice treated with (4NQO + calcitriol → calcitriol) compared to 4NQO controls (77 pg/ml) and the two calcitriol regimens, 4NQO + calcitriol (62 pg/ml) and 4NQO → calcitriol (70 pg/ml) (Figure 3*C*). Given the risk of

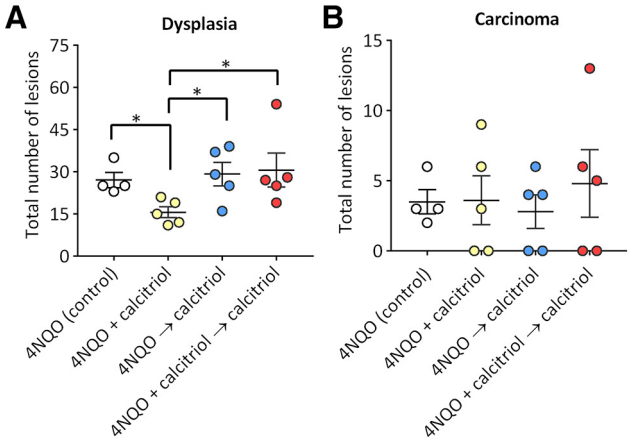

Figure 5. Histopathologic evaluation of the effects of calcitriol on oral premalignant lesions and SCC. Incidence of oral dysplasia (**A**) and carcinomas (**B**) in control and calcitriol treated mice. Groups: Control: 4NQO only (White circles); calcitriol administered for 16 weeks concurrently with 4NQO exposure (4NQO + calcitriol; yellow circles), calcitriol administered for 10 weeks post completion of 4NQO exposure (4NQO → calcitriol; blue circles), and calcitriol administered for a period of 26 weeks, concurrent with and following 4NQO exposure (4NQO + calcitriol → calcitriol; Red circles). Values represent mean ± standard error of mean. *$P < .05$.

hypercalcemia with calcitriol administration, we measured serum calcium by colorimetry which showed calcium levels to be within the normal range of 8–10 mg/dl in mice [30] across the groups (Figure 3*D*).

MRI-based Monitoring of 4NQO-Induced Oral Lesions in Mice

We utilized non-invasive MRI to longitudinally monitor changes in the oral cavity of mice following exposure to 4NQO with or without calcitriol treatment over 26 weeks. The panel of images shown in Figure 4 represent non-contrast enhanced T2-weighted MR images of the region-of-interest (oral cavity) from an animal in each of the 4 groups at week 0 (prior to 4NQO exposure), week 16 (following completion of 4NQO exposure) and at weeks 20, 24 and 26 (study end point). Whole axial slices of the animals from the 4 groups are shown in Supplementary Figure S2. MRI examination of all five animals in the 4NQO control group showed evidence of hyperintense thickening (4NQO; *outlined in yellow*) of the lateral borders of the tongue by week 16 suggestive of early hyperplastic changes following carcinogen exposure.

Exophytic lesions on the tongues of mice were detected by week 20 suggestive of malignant transformation. In comparison, animals in the 4NQO + calcitriol group showed thickening of lateral borders of the tongue (*white arrows*) without any evidence of exophytic growth. Similar to the control animals, animals in the two calcitriol regimens (4NQO → calcitriol, (4NQO + calcitriol → calcitriol) showed evidence of lesions on lateral borders and anterior tongue (*white* arrows) or exophytic lesions on the dorsum (*yellow outline*) visible on MRI.

Efficacy of Calcitriol Administration on Oral Dysplasia and SCC

Next, we evaluated the effect of the stage of intervention and duration of calcitriol on the oral dysplasia and SCC by histologic evaluation (Figure 5). Whole tongue sections from control animals (4NQO alone) and mice exposed to the three calcitriol regimens were evaluated at week 26 (study end point). The incidence of low grade dysplasia was comparable between 4NQO controls (100%) and the three calcitriol regimens (80–100%). Two out of 4 animals (50%) in the control group showed high grade dysplasia while 1/5 (20%) animals in the 4NQO + calcitriol group, 4/5 (80%) animals in the 4NQO → calcitriol and 4/5 (80%) animals in the 4NQO + calcitriol → calcitriol showed presence of high grade dysplastic lesions. These differences were not statistically significant. Quantitative analysis (Figure 5*A*) revealed a significant decrease in the number of dysplastic lesions in the 4NQO + calcitriol group (15.6 ± 1.94) compared to 4NQO alone controls (27.0 ± 2.71, $P = .01$), 4NQO → calcitriol (29.2 ± 4.18; $P = .031$) and 4NQO + calcitriol → calcitriol (30.6 ± 6.06; $P = .020$). Histologic evaluation revealed presence of SCC in 4/4 (100%) of 4NQO control animals with 1/4 mice (25%) exhibiting invasive SCC. In comparison, only 60% of animals in the three calcitriol regimens showed presence of SCC. Notably, none of the animals (0/5) in the 4NQO + calcitriol group showed evidence of invasive SCC. One out of five animals (20%) in the 4NQO → calcitriol group showed SCC that was invasive while 3/5 (60%) animals in 4NQO + calcitriol → calcitriol showed evidence of invasive SCC. Evaluation of tumor multiplicity (Figure 5*B*) did not reveal any significant difference between 4NQO controls (3.5 ± 0.87) and the three calcitriol regimens: 4NQO + calcitriol (3.6 ± 1.7), 4NQO → calcitriol (2.8 ± 1.2), 4NQO + calcitriol → calcitriol (4.8 ± 2.4).

Impact of Calcitriol Intervention on Disease Phenotype and Vitamin D Signaling

Finally, we examined the effect of calcitriol treatment on disease phenotype. To accomplish this, tongue sections from control and calcitriol treated mice excised at week 26 were immunostained for the proliferation marker, Ki67. The biological effects of calcitriol are mediated through its interactions with the vitamin D receptor (VDR) and regulated by local levels of the hydroxylase CYP24A1 in target tissues. Therefore, in addition to Ki67, tongues were immunostained for VDR and CYP24A1 to evaluate the impact of the three calcitriol regimens on local vitamin D signaling. The panel of images shown in Figure 6 represent photomicrographs of hematoxylin and eosin stained tongue sections (H&E) along with matched fields of VDR and CYP24A1 (10X magnification). Corresponding Ki67 immunostained field (40X) magnification is also shown on the right. The images for the control (4NQO alone) and the three calcitriol regimens are shown for normal tongue epithelium (**A**), low-grade dysplasia (**B**), high-grade dysplasia (**C**), and invasive cancer (**D**). Quantification of VDR, CYP24A1 and Ki67 levels across the groups and disease stages are presented in Figure 7. Control animals (4NQO alone) and animals treated with the two calcitriol regimens, 4NQO → calcitriol and 4NQO+ calcitriol → calcitriol showed presence of invasive SCC (Figure 6*D*) while the worst histologic diagnosis in animals exposed to 4NQO + calcitriol was high grade dysplasia (Figure 6*C*). Protein expression of VDR, CYP24A1 and Ki67 was detectable in all normal epithelium, LGD, HGD and OSCC across the 4 groups (Figure 6, *A–D*). Control tongues showed higher nuclear VDR staining in high-grade dysplasia ($P < .001$) and OSCC ($P < .05$) compared to normal epithelium (Figure 7*A*). A significant ($P < .01$) increase in VDR staining was also seen in high grade dysplastic lesions compared to low grade lesions in control animals (Figure 7*A*). Tongues of mice from 4NQO + calcitriol (Figure 7*B*) and 4NQO → calcitriol (Figure 7*C*) cohorts showed a significant increase in VDR in high grade dysplasia compared to normal epithelium. No difference in VDR staining intensity was seen between normal epithelium and diseased tongue in animals in the 4NQO + calcitriol → calcitriol group (Figure 7*D*).

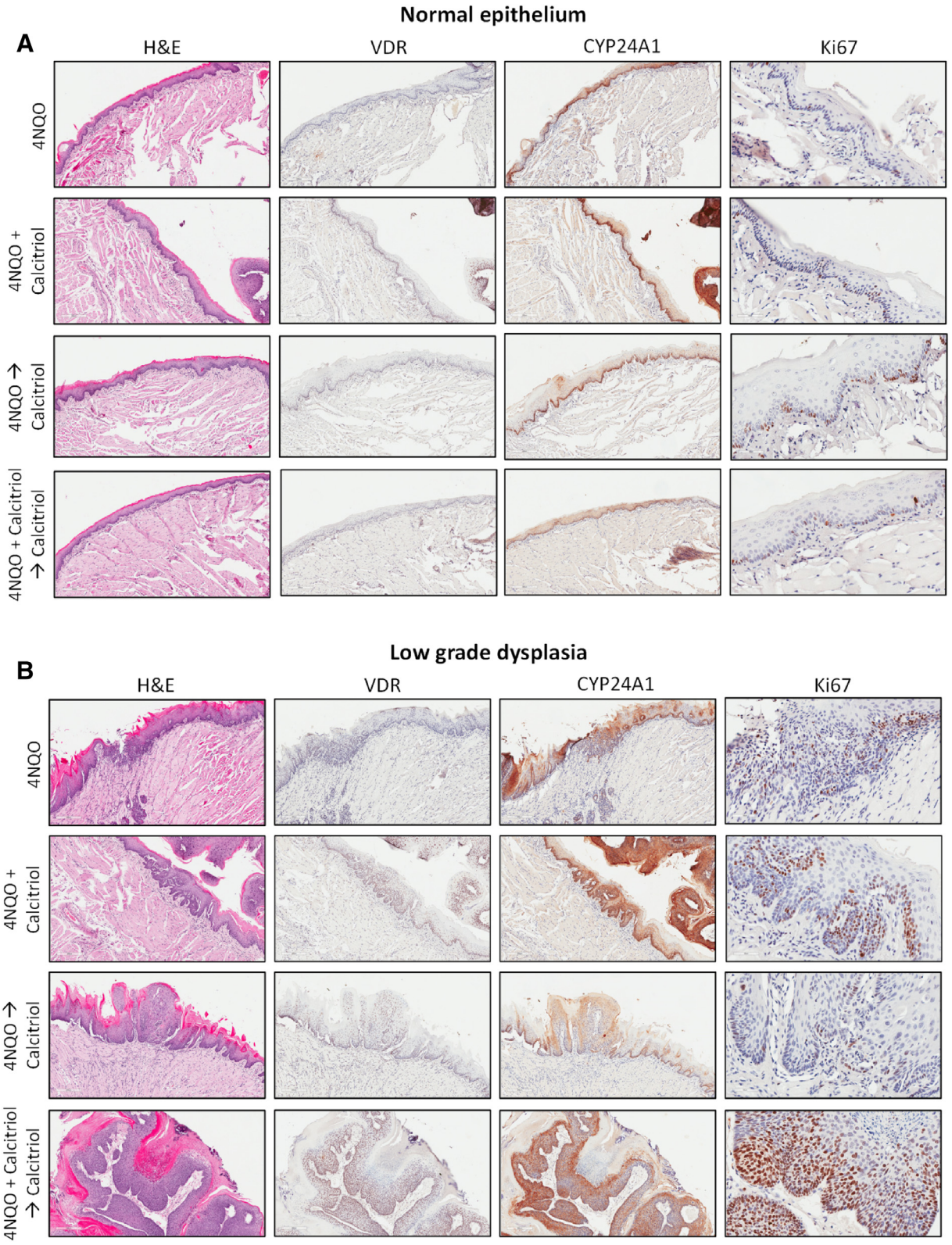

Figure 6. Impact of calcitriol intervention on disease phenotype and vitamin D signaling. The panel of images represent photomicrographs of hematoxylin and eosin stained tongue sections (H&E) along with matched fields of VDR and CYP24A1 (10X magnification). Corresponding Ki67 immunostained field (40X) magnification is also shown on the right. The images for the control (4NQO alone) and the three calcitriol regimens have been shown for normal tongue epithelium (**A**), low-grade dysplasia (**B**), high-grade dysplasia (**C**), and invasive cancer (**D**).

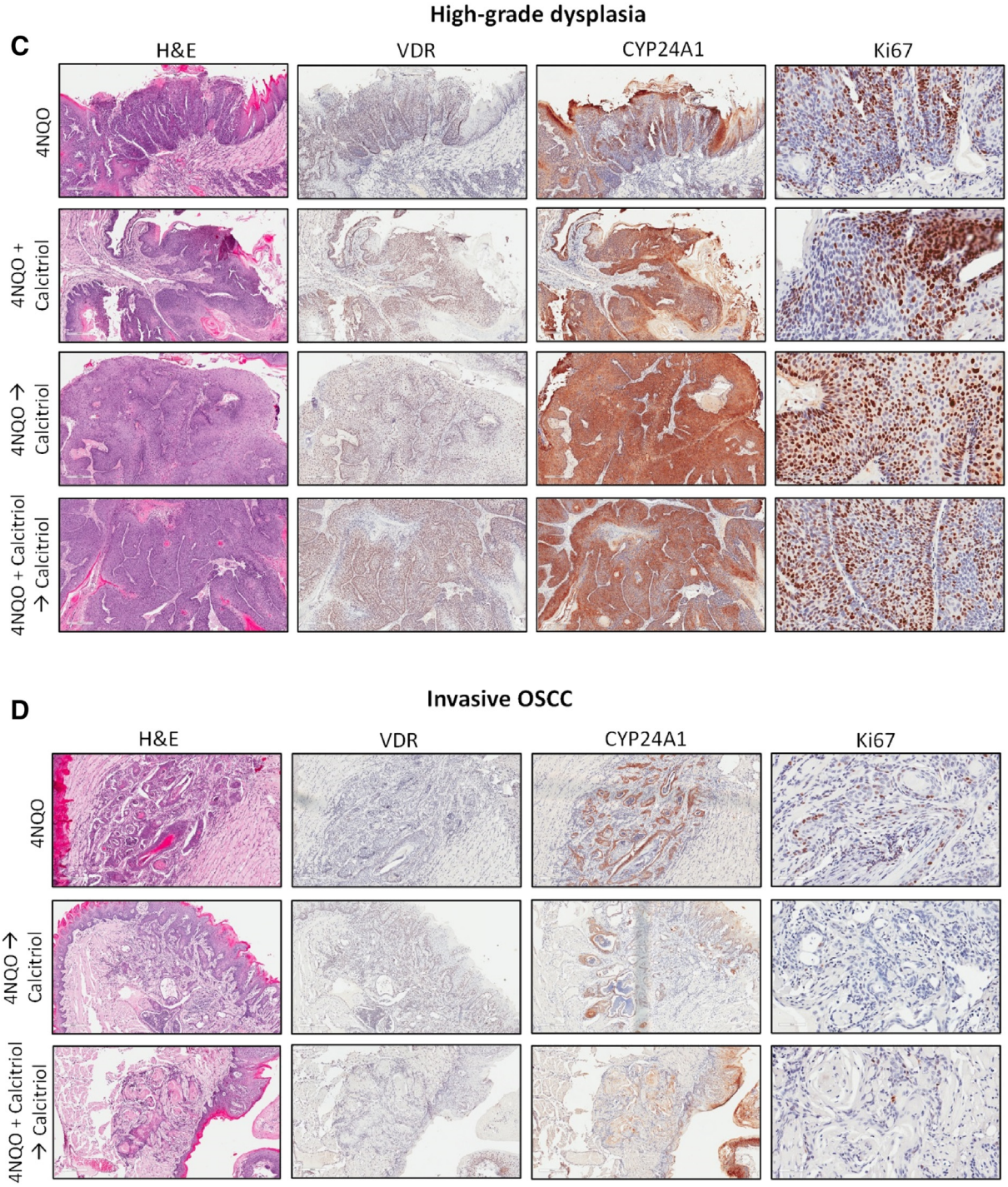

Fig. 6 (*continued*).

CYP24A1 immunostained tongue sections from 4NQO control animals (Figures 6, *A–D* and 7*E*) and animals in 4NQO + calcitriol → calcitriol group (Figure 7*H*) did not show any differences across the disease spectrum compared to normal epithelium. Both low-grade and high-grade dysplastic lesions showed increased CYP24A1 staining compared to normal epithelium (Figure 7*F*) in animals treated with 4NQO + calcitriol. In comparison, areas with high grade dysplasia alone showed increased CYP24A1 staining compared to normal epithelium in the 4NQO → calcitriol group (Figure 7*G*). Ki67 immunostaining revealed positive nuclear staining in all 4 groups from normal epithelium to invasive cancer. Control (4NQO) animals showed increased Ki67 scores in dysplastic and invasive OSCC compared to normal epithelium (Figures 6, *A–D*, 7*I*). Similarly, animals treated with 4NQO + calcitriol (Figure 7*J*) and 4NQO → calcitriol (Figure 7*K*) showed increased Ki67 levels in low-grade and high-grade dysplastic lesions compared to normal epithelium. Tongues from animals exposed to 4NQO + calcitriol → calcitriol showed comparable staining across dysplastic and invasive OSCC (Figure 7*L*).

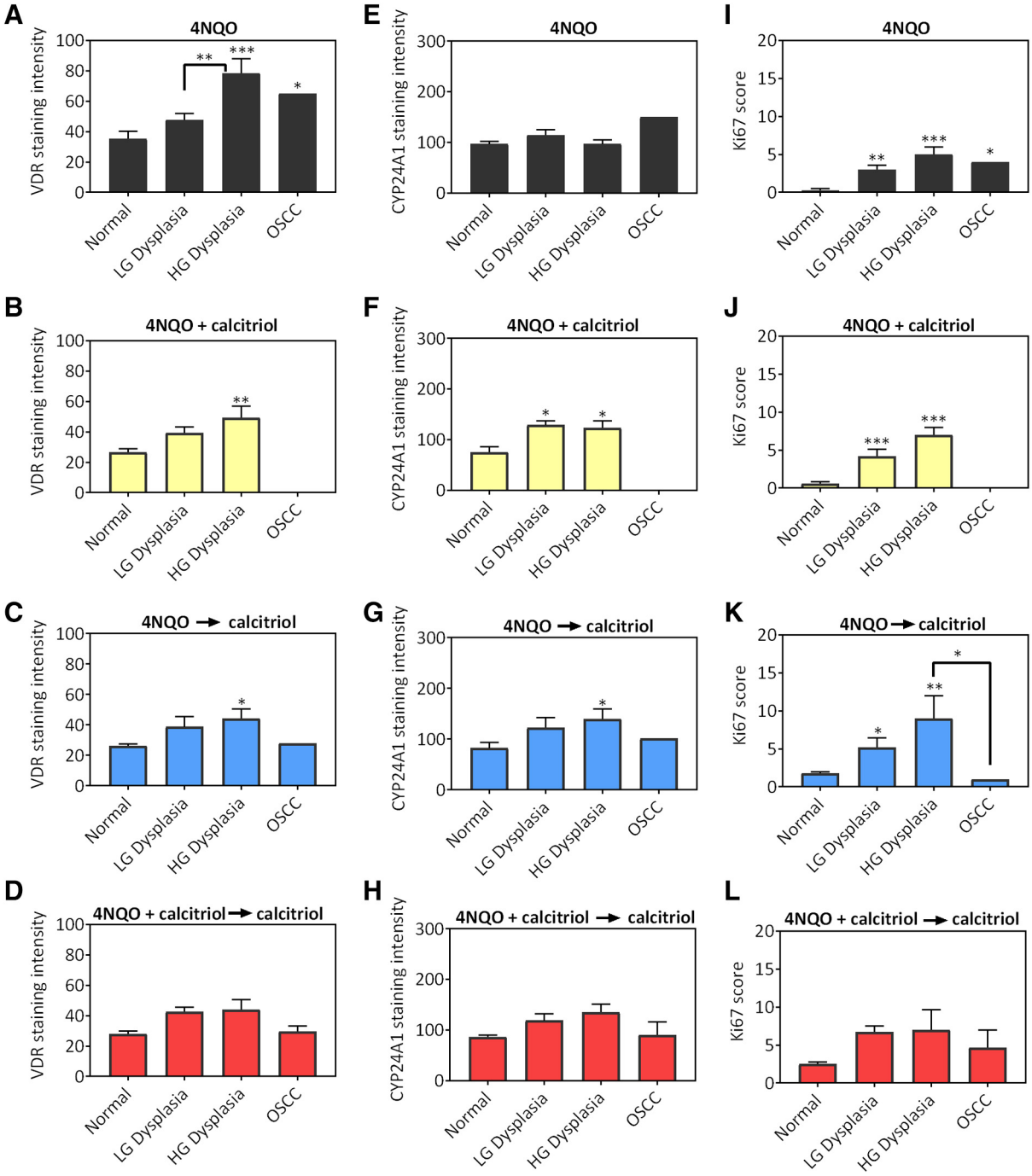

Figure 7. Change in VDR immunostaining in tongue lesions from 4NQO exposed mice treated with calcitriol. Bar graphs show quantitative estimates of VDR staining intensity (**A-D**), CYP24A1 (**E-H**), and Ki67 scores (**I-L**)in normal epithelium, low grade dysplasia (LG dysplasia), High grade dysplasia (HD dysplasia) and OSCC for control (4NQO), 4NQO + calcitriol (**B**) 4NQO → calcitriol (**C**) 4NQO + calcitriol → calcitriol (**D**) treated animals. Values represent mean ± standard error of mean. *$P < .05$; **$P < .01$, ***$P < .001$.

Discussion

Successful development of safe and effective preventive strategies could have a significant impact on the quality of life and survival of OSCC patients. Oral cancers are considered an ideal disease site for preventive intervention given that the oral cavity is an easily accessible site for clinical examination and histologic evaluation of suspicious lesions. The ease of access to diseased sites combined with modifiable risk factors (tobacco and alcohol use) and unique disease biology (field cancerization) has led to widespread interest in evaluating nutritional supplements and plant extracts for their potential chemopreventive activity against oral premalignant and malignant lesions. In this regard, several studies have shown that vitamin D and its analogues exhibit potent growth inhibitory effects against oral cancer cells in culture [24,25]. Studies have also demonstrated the potential antitumor activity of vitamin D *in vivo* using experimental models of oral cancers [22,23]. Using the Syrian hamster buccal carcinoma model, Meier and colleagues showed that administration of calcitriol significantly inhibited the development of oral neoplastic lesions

following exposure to the carcinogen, 7,12-dimethylbenzanthracene (DMBA) over a 14 week period [22]. In the 4NQO model, we have previously demonstrated that administration of calcitriol for 4 weeks can enhance the activity of the EGFR inhibitor, Erlotinib, against OSCC [23]. However, the activity of vitamin D against the spectrum of oral carcinogenesis has not been previously reported. To address this gap in knowledge, we conducted preclinical trials to answer two questions integral to the clinical implementation of preventive regimens: Is long-term administration of calcitriol safe and effective in preventing oral carcinogenesis? Does the stage of intervention affect the chemopreventive activity (inhibition of initiation *vs.* inhibition of progression) of calcitriol?

We employed the 4NQO carcinogen-induced murine model of OSCC to determine the impact of disease stage and duration of exposure on the chemopreventive efficacy of calcitriol against OSCC. 4NQO is a synthetic water-soluble carcinogen that mimics the effects of chronic tobacco use [26,31]. Chronic exposure of mice and rats to 4NQO in drinking water results in histologic and molecular alterations similar to human OSCC through intracellular oxidative stress and formation of DNA adducts [31,32]. The 4NQO OSCC model shares several pathologic and molecular features of human OSCC and has been widely used for preclinical evaluation of chemopreventive agents [23,26,27]. Systemic long-term administration of calcitriol in this model was well tolerated with no significant change in body weight observed between the control and treatment groups. We examined the effects of the three calcitriol regimens on vitamin D metabolism and calcium homeostasis in mice. We observed a negative correlation between serum $1,25(OH)_2D3$ levels and duration of calcitriol treatment (Supplementary Figure S3). While serum 25 $(OH)D_3$ levels were comparable between control and calcitriol treated animals, mice treated with calcitriol for 26 weeks (4NQO + calcitriol → calcitriol) showed lowest serum 1,25 $(OH)_2D_3$ suggestive of suppression of vitamin D activity, consistent with a previous report by Fleet et al. [33]. Given the risk of hypercalcemia associated with chronic calcitriol administration, we examined serum calcium levels in mice treated with the three calcitriol regimens. Serum calcium levels in control and calcitriol-treated animals using all three regimens were comparable and within the normal range [30].

We utilized non-invasive MRI to monitor the course of disease progression in the 4NQO model. Serial MRI performed at regular intervals prior to, during and after carcinogen exposure and calcitriol treatment enabled longitudinal *in vivo* monitoring of oral carcinogenesis. Early evidence of preneoplastic changes in the oral cavity (hyperintense tongue lesions on T2W images) was detected by MRI examination at week 16 with exophytic lesions detected by week 24. Notably, none of the animals in the 4NQO + calcitriol group showed evidence of exophytic masses indicative of inhibition of malignant transformation with this regimen. Longitudinal MRI examination did not reveal any differences in the onset of exophytic lesions between control and the two other calcitriol regimens. This suggests that prolonged administration of calcitriol (4NQO + calcitriol → calcitriol) or administration of calcitriol following carcinogen exposure (4NQO → calcitriol) is ineffective in inhibiting disease progression or promotion in the 4NQO model. This is consistent with our previous study in which we observed minimal growth inhibition with short-term calcitriol treatment administered following carcinogen exposure in the 4NQO model [23]. The changes that contribute to the increased contrast in these oral lesions compared to surrounding tongue is unclear. Ongoing studies in the laboratory are examining the epithelial, stromal and vascular changes in response to 4NQO through functional imaging methods including T1, T2 mapping and diffusion weight imaging. Given the ability of MRI to allow for temporal examination of individual lesions, it would also be interesting to examine the histologic and molecular differences between progressing and non-progressing oral lesions using laser capture microdissection. Consistent with the MRI findings, histologic evaluation revealed that administration of calcitriol concurrently with 4NQO exposure for 16 weeks significantly reduced the incidence of premalignant lesions and inhibited malignant transformation (0/5 animals showed invasive cancer on histologic examination). Although the mechanism behind this observation is not clear, 4NQO results in the formation of DNA adducts such as 8-hydroxydeoxyguanosine (8OHdG) as a result of oxidative stress [26,31,32]. In this regard, vitamin D metabolites have previously been shown to decrease oxidative stress by reducing 8OHdG in colon cancer [34]. It is therefore plausible that administration of vitamin D concurrently with carcinogen exposure decreases carcinogen-induced oxidative stress during the tumor initiation phase. Our findings are in agreement with a previous report by Ajibade et al. [20] in which calcitriol was shown to be effective in inhibiting early stage disease in the transgenic adenocarcinoma of the mouse prostate (TRAMP) model. While all 3 calcitriol regimens resulted in a reduction in the incidence of carcinomas (60%) compared to 4NQO controls (100%), we observed an increase in the incidence of invasive cancer (3/5; 60%) in animals treated with calcitriol for 26 weeks compared to 4NQO controls (1/4; 25%). To explain this observation, we examined the impact of the three calcitriol regimens on vitamin D homeostasis. Since catabolic inactivation of calcitriol to $1,24,25\ (OH)_2D_3$ occurs in the kidneys by CYP24A1, we compared renal CYP24A1 mRNA levels in mice exposed to the three different calcitriol regimens. Normalized expression levels of CYP24A1 mRNA showed ~3-fold increase in mice exposed to calcitriol for 26 weeks (4NQO + calcitriol → calcitriol) compared to 4NQO controls (Supplementary Figure S4). A positive correlation was observed between the duration of calcitriol exposure and renal mRNA CYP24A1 levels (Pearson's correlation r = 0.99; P = .008) (Supplementary Figure S5). Analysis of renal CYP27B1 did not show any significant difference across the groups (Supplementary Figure S4).

Given that local (tongue) levels of CYP24A1 are likely to be a critical determinant of the anticancer activity of calcitriol, we performed immunostaining of tongue sections for CYP24A1 in the context of VDR signaling and disease phenotype (Ki67). We observed increased VDR expression in high grade dysplasia and SCC compared to normal epithelium. This is consistent with a previous observation by Grimm et al. [35] in human oral precancerous lesions and OSCC. Although the mechanisms behind this overexpression in early stages of oral carcinogenesis are unclear, it is plausible that the gradual increase in VDR expression in dysplastic epithelium is related to the increased number of proliferating cells. We observed a reduction in VDR expression following calcitriol treatment which is in agreement with previous studies [23]. The downregulation of VDR protein expression could be attributed to the high levels of CYP24A1 induced by calcitriol which leads to increased metabolism of the VDR ligand, $1,25(OH)_2D_3$ [36]. Compared to normal epithelium, increased CYP24A1 expression was seen in dysplastic lesions of mice treated with 4NQO + calcitriol or 4NQO → calcitriol. No difference in CYP24A1 expression was observed in mice exposed to 4NQO alone or 4NQO + calcitriol → calcitriol. This suggests that increased tumorigenesis in animals chronically exposed to calcitriol (26 weeks) is unlikely due to a change in local catabolism of calcitriol. While studies have previously reported upregulation of CYP24A1 in breast and colon cancers compared to normal tissues [37,38], our results highlight the potential of CYP24A1

as a potential early marker of dysregulation in vitamin D signaling during oral carcinogenesis.

And finally, examination of the disease phenotype showed increased Ki67 staining in dysplastic compared to normal epithelium in control animals and animals treated with 4NQO + calcitriol or 4NQO → calcitriol. In contrast, tongues from animals exposed to 4NQO + calcitriol → calcitriol did not show any difference in Ki67 staining between healthy and diseased tissue. Notably, higher Ki67 staining was seen even in the normal epithelium of mice exposed to this calcitriol regimen compared to all other groups. In this regard, Yuan et al. have shown that vitamin D deficient mice with decreased serum $25D_3$ exhibit increased proliferation of the tongue epithelium [39]. It is therefore possible that chronic exposure to calcitriol results in high renal CYP24A1 induction and decreased systemic 1, $25(OH)_2D_3$ levels, which contributes to increased proliferation in healthy and diseased epithelial tissues.

In summary, our studies demonstrate that the effects of calcitriol on oral carcinogenesis are critically influenced by the stage of intervention and duration of exposure. Although limited by the small sample size, our observations suggest that calcitriol treatment during carcinogen exposure could be beneficial in halting malignant transformation of oral premalignant lesions, while chronic administration of calcitriol could potentially enhance carcinogenesis by sustained induction of CYP24A1 and suppression of endogenous $1,25(OH)_2D_3$ levels. However, several questions remain to be answered. First, given the limited sample size for individual cohorts in our study, future studies could examine the activity of calcitriol on disease progression using a large cohort of animals of both sexes over longer periods of observation. It would also be important to evaluate the effects of vitamin D in the context of young and old animals. It should be noted that animals in our study were maintained on a Vitamin D replete diet (house chow diet that contained 1000 IU Vitamin D). It would therefore be important to examine how calcitriol administration affects oral carcinogenesis in the context of vitamin D deficiency. It would also be useful to determine if dietary vitamin D supplementation is a better alternative for safe and sustained production of $1,25(OH)_2D_3$. These studies may assist in determining the best intervention stage and duration of exposure of calcitriol for patients with premalignant lesions. Assessment of vitamin D status in patients with oral premalignant lesions and invasive cancer will also enable development of tailored vitamin D supplementation regimens that exhibit maximal chemopreventive efficacy. We have begun designing studies to address these questions and will report on our findings in the future.

Acknowledgements

This work was supported by grants R01DE024595 from the National Institute of Dental and Craniofacial Research, Roswell Park Alliance Foundation and utilized shared resources supported by Roswell Park Comprehensive Cancer Center Support Grant from the National Cancer Institute P30CA06156 (C. S. Johnson). The authors would like to thank staff members of the following shared resources at RPCI for their technical support in conducting the experimental studies presented in this manuscript - Translational Imaging Resource, Laboratory Animal Resource, and the Pathology Resource Network. The authors do not have any conflicts to disclose. The funding sponsors had no role in the design of the study, collection, analyses or interpretation of the data, writing of the manuscript and the decision to publish the results.

Conflicts of Interest

The authors declare that no competing interests exist.

Appendix A. Supplementary data

Supplementary data to this article can be found online at https://doi.org/10.1016/j.neo.2019.02.002.

References

[1] Johnson NW (1991). Orofacial neoplasms: global epidemiology, risk factors and recommendations for research. *Int Dent J* **41**, 365–375.
[2] Warnakulasuriya S (2009). Global epidemiology of oral and oropharyngeal cancer. *Oral Oncol* **45**, 309–316.
[3] Brown KS and Kane MA (2006). Chemoprevention of squamous cell carcinoma of the oral cavity. *Otolaryngol Clin North Am* **39**, 349–363.
[4] Choi S and Myers JN (2008). Molecular pathogenesis of oral squamous cell carcinoma: implications for therapy. *J Dent Res* **87**, 14–32.
[5] Day GL and Blot WJ (1992). Second primary tumors in patients with oral cancer. *Cancer* **70**, 14–19.
[6] Christakos S, Ajibade DV, Dhawan P, Fechner AJ, and Mady LJ (2010). Vitamin D: metabolism. *Endocrinol Metab Clin North Am* **39**, 243–253 [table of contents].
[7] Veldurthy V, Wei R, Campbell M, Lupicki K, Dhawan P, and Christakos S (2016). 25-Hydroxyvitamin D(3) 24-Hydroxylase: A Key Regulator of 1,25(OH)(2)D(3) Catabolism and Calcium Homeostasis. *Vitam Horm* **100**, 137–150.
[8] Pike JW and Meyer MB (2012). Regulation of mouse Cyp24a1 expression via promoter-proximal and downstream-distal enhancers highlights new concepts of 1,25-dihydroxyvitamin D(3) action. *Arch Biochem Biophys* **523**, 2–8.
[9] Zierold C, Darwish HM, and DeLuca HF (1995). Two vitamin D response elements function in the rat 1,25-dihydroxyvitamin D 24-hydroxylase. promoter. *J Biol Chem* **270**, 1675–1678.
[10] Bartonkova I, Kallay E, and Dvorak Z (2018). Effects of human interleukins in the transgenic gene reporter cell lines IZ-VDRE and IZ-CYP24 designed to assess the transcriptional activity of vitamin D receptor. *PLoS One* **13**e0193655.
[11] Chen S, Sun Y, and Agrawal DK (2015). Vitamin D deficiency and essential hypertension. *J Am Soc Hypertens* **9**, 885–901.
[12] Grammatiki M, Rapti E, Karras S, Ajjan RA, and Kotsa K (2017). Vitamin D and diabetes mellitus: Causal or casual association? *Rev Endocr Metab Disord* **18**, 227–241.
[13] Feldman D, Krishnan AV, Swami S, Giovannucci E, and Feldman BJ (2014). The role of vitamin D in reducing cancer risk and progression. *Nat Rev Cancer* **14**, 342–357.
[14] Gupta D, Vashi PG, Trukova K, Lis CG, and Lammersfeld CA (2011). Prevalence of serum vitamin D deficiency and insufficiency in cancer: Review of the epidemiological literature. *Exp Ther Med* **2**, 181–193.
[15] Fanidi A, Muller DC, Midttun O, Ueland PM, Vollset SE, Relton C, Vineis P, Weiderpass E, Skeie G, and Brustad M, et al (2016). Circulating vitamin D in relation to cancer incidence and survival of the head and neck and oesophagus in the EPIC cohort. *Sci Rep* **6**36017.
[16] Orell-Kotikangas H, Schwab U, Österlund P, Saarilahti K, Mäkitie O, and Mäkitie AA (2012). High prevalence of vitamin D insufficiency in patients with head and neck cancer at diagnosis. *Head Neck* **34**, 1450–1455.
[17] Johnson CS, Muindi JR, Hershberger PA, and Trump DL (2006). The antitumor efficacy of calcitriol: preclinical studies. *Anticancer Res* **26**, 2543–2549.
[18] Deeb KK, Trump DL, and Johnson CS (2007). Vitamin D signalling pathways in cancer: potential for anticancer therapeutics. *Nat Rev Cancer* **7**, 684–700.
[19] Jeong Y, Swami S, Krishnan AV, Williams JD, Martin S, Horst RL, Albertelli MA, Feldman BJ, Feldman D, and Diehn M (2015). Inhibition of Mouse Breast Tumor-Initiating Cells by Calcitriol and Dietary Vitamin D. *Mol Cancer Ther* **14**, 1951–1961.
[20] Ajibade AA, Kirk JS, Karasik E, Gillard B, Moser MT, Johnson CS, Trump DL, and Foster BA (2014). Early growth inhibition is followed by increased metastatic disease with vitamin D (calcitriol) treatment in the TRAMP model of prostate cancer. *PLoS One* **9**e89555.
[21] Mazzilli SA, Hershberger PA, Reid ME, Bogner PN, Atwood K, Trump DL, and Johnson CS (2015). Vitamin D Repletion Reduces the Progression of Premalignant Squamous Lesions in the NTCU Lung Squamous Cell Carcinoma Mouse Model. *Cancer Prev Res (Phila)* **8**, 895–904.
[22] Meier JD, Enepekides DJ, Poirier B, Bradley CA, Albala JS, and Farwell DG (2007). Treatment with 1-alpha,25-dihydroxyvitamin D3 (vitamin D3) to inhibit carcinogenesis in the hamster buccal pouch model. *Arch Otolaryngol Head Neck Surg* **133**, 1149–1152.
[23] Bothwell KD, Shaurova T, Merzianu M, Suresh A, Kuriakose MA, Johnson CS, Hershberger PA, and Seshadri M (2015). Impact of Short-term 1,25-Dihydroxyvitamin D3 on the Chemopreventive Efficacy of Erlotinib against Oral Cancer. *Cancer Prev Res (Phila)* **8**, 765–776.

[24] Hager G, Formanek M, Gedlicka C, Thurnher D, Knerer B, and Kornfehl J (2001). 1,25(OH)2 vitamin D3 induces elevated expression of the cell cycle-regulating genes P21 and P27 in squamous carcinoma cell lines of the head and neck. *Acta Otolaryngol* **121**, 103–109.

[25] Gedlicka C, Hager G, Weissenbock M, Gedlicka W, Knerer B, Kornfehl J, and Formanek M (2006). 1,25(OH)2Vitamin D3 induces elevated expression of the cell cycle inhibitor p18 in a squamous cell carcinoma cell line of the head and neck. *J Oral Pathol Med* **35**, 472–478.

[26] Kanojia D and Vaidya MM (2006). 4-nitroquinoline-1-oxide induced experimental oral carcinogenesis. *Oral Oncol* **42**, 655–667.

[27] Zhou G, Hasina R, Wroblewski K, Mankame TP, Doci CL, and Lingen MW (2010). Dual inhibition of vascular endothelial growth factor receptor and epidermal growth factor receptor is an effective chemopreventive strategy in the mouse 4-NQO model of oral carcinogenesis. *Cancer Prev Res (Phila)* **3**, 1493–1502.

[28] Warnakulasuriya S (2001). Histological grading of oral epithelial dysplasia: revisited. *J Pathol* **194**, 294–297.

[29] Warnakulasuriya S, Reibel J, Bouquot J, and Dabelsteen E (2008). Oral epithelial dysplasia classification systems: predictive value, utility, weaknesses and scope for improvement. *J Oral Pathol Med* **37**, 127–133.

[30] Smith EA, Frankenburg EP, Goldstein SA, Koshizuka K, Elstner E, Said J, Kubota T, Uskokovic M, and Koeffler HP (2000). Effects of long-term administration of vitamin D3 analogs to mice. *J Endocrinol* **165**, 163–172.

[31] Ikenaga M, Ishii Y, Tada M, Kakunaga T, and Takebe H (1975). Excision-repair of 4-nitroquinolin-1-oxide damage responsible for killing, mutation, and cancer. *Basic Life Sci* **5B**, 763–771.

[32] Arima Y, Nishigori C, Takeuchi T, Oka S, Morimoto K, Utani A, and Miyachi Y (2006). 4-Nitroquinoline 1-oxide forms 8-hydroxydeoxyguanosine in human fibroblasts through reactive oxygen species. *Toxicol Sci* **91**, 382–392.

[33] Fleet JC, Gliniak C, Zhang Z, Xue Y, Smith KB, McCreedy R, and Adedokun SA (2008). Serum metabolite profiles and target tissue gene expression define the effect of cholecalciferol intake on calcium metabolism in rats and mice. *J Nutr* **138**, 1114–1120.

[34] Bostick RM (2015). Effects of supplemental vitamin D and calcium on normal colon tissue and circulating biomarkers of risk for colorectal neoplasms. *J Steroid Biochem Mol Biol* **148**, 86–95.

[35] Grimm M, Cetindis M, Biegner T, Lehman M, Munz A, Teriete P, and Reinert S (2015). Serum vitamin D levels of patients with oral squamous cell carcinoma (OSCC) and expression of vitamin D receptor in oral precancerous lesions and OSCC. *Med Oral Patol Oral Cir Bucal* **20**, e188–e195.

[36] Wiese RJ, Uhland-Smith A, Ross TK, Prahl JM, and DeLuca HF (1992). Up-regulation of the vitamin D receptor in response to 1,25-dihydroxyvitamin D3 results from ligand-induced stabilization. *J Biol Chem* **267**, 20082–20086.

[37] Anderson MG, Nakane M, Ruan X, Kroeger PE, and Wu-Wong JR (2006). Expression of VDR and CYP24A1 mRNA in human tumors. *Cancer Chemother Pharmacol* **57**, 234–240.

[38] Zhalehjoo N, Shakiba Y, and Panjehpour M (2017). Gene expression profiles of CYP24A1 and CYP27B1 in malignant and normal breast tissues. *Mol Med Rep* **15**, 467–473.

[39] Yuan FN, Valiyaparambil J, Woods MC, Tran H, Pant R, Adams JS, and Mallya SM (2014). Vitamin D signaling regulates oral keratinocyte proliferation in vitro and in vivo. *Int J Oncol* **44**, 1625–1633.